Progression from a stem cell–like state to early differentiation in the *C. elegans* germ line

Olivier Cinquin[a,b,1,2], Sarah L. Crittenden[a,1], Dyan E. Morgan[c], and Judith Kimble[a,c,d,2]

[a]Howard Hughes Medical Institute, [c]Program in Cellular and Molecular Biology, and [d]Department of Biochemistry, University of Wisconsin, Madison, WI 53706; and [b]Department of Developmental and Cell Biology and Center for Complex Biological Systems, University of California, Irvine, CA 92697

Contributed by Judith Kimble, November 3, 2009 (sent for review August 18, 2009)

Controls of stem cell maintenance and early differentiation are known in several systems. However, the progression from stem cell self-renewal to overt signs of early differentiation is a poorly understood but important problem in stem cell biology. The *Caenorhabditis elegans* germ line provides a genetically defined model for studying that progression. In this system, a single-celled mesenchymal niche, the distal tip cell (DTC), employs GLP-1/Notch signaling and an RNA regulatory network to balance self-renewal and early differentiation within the "mitotic region," which continuously self-renews while generating new gametes. Here, we investigate germ cells in the mitotic region for their capacity to differentiate and their state of maturation. Two distinct pools emerge. The "distal pool" is maintained by the DTC in an essentially uniform and immature or "stem cell–like" state; the "proximal pool," by contrast, contains cells that are maturing toward early differentiation and are likely transit-amplifying cells. A rough estimate of pool sizes is 30–70 germ cells in the distal immature pool and ≈150 in the proximal transit-amplifying pool. We present a simple model for how the network underlying the switch between self-renewal and early differentiation may be acting in these two pools. According to our model, the self-renewal mode of the network maintains the distal pool in an immature state, whereas the transition between self-renewal and early differentiation modes of the network underlies the graded maturation of germ cells in the proximal pool. We discuss implications of this model for controls of stem cells more broadly.

stem cell niche | self-renewal | transit amplification | network dynamics | developmental timing

Stem cells generate tissues during development and maintain them in adults. The stem cell niche is an important and well-characterized regulator of stem cells. Signaling from the niche maintains stem cells in a stem cell state, whereas movement from the niche occurs as stem cell daughters mature and begin the path toward differentiation (e.g., refs. 1 and 2). One simple model has been that niche signaling controls asymmetric cell division so that stem cells produce one stem cell daughter and one daughter destined to differentiate (3). According to this model, tissue homeostasis is controlled at the level of individual cells. Alternatively, homeostasis can be controlled at a population level (2, 4). Although superficially distinct, these two stem cell systems could be controlled by a similar underlying regulatory logic.

Caenorhabditis elegans germ-line stem cells are regulated as a population (4, 5). In this system, a single mesenchymal cell, the distal tip cell (DTC), provides the stem cell niche and maintains a group of ≈200 mitotically dividing cells within the "mitotic region" at the distal end of the gonad (Fig. 1 *A* and *B*). This mitotic region is essential for germ-line self-renewal (5–7). As germ cells move proximally out of the mitotic region, they enter early meiotic prophase (Fig. 1 *A* and *B*); more proximally, they progress through meiotic prophase and ultimately make gametes near the proximal end of the gonad. Germ "cells" are interconnected via a common cytoplasmic core and they are likely to move proximally as a group (7, 8). Because the distal-most germ cells have no additional input from more distal cells, they are inferred to be the "actual" stem cells, which are defined as those that actually make more stem cells and also generate differentiated progeny (7, 9, 10) (Fig. 1*A*).

A well-defined regulatory network controls the balance between germ-line self-renewal and early differentiation (meiotic entry) (5) (Fig. 1*C*). Regulators that promote self-renewal include GLP-1/Notch signaling and two nearly identical Pumilio and FBF (PUF) RNA-binding proteins (11–13). Regulators that promote meiotic entry include three GLD proteins that regulate RNA (14–22). Germ-line self-renewal is eliminated when the network becomes unbalanced by a loss of mitosis-promoting factors (11, 12); by contrast, germ-line tumors arise when the network becomes unbalanced by either deregulation of mitosis-promoting factors or removal of meiosis-promoting factors (15, 16, 23, 24). Importantly, both Notch signaling and PUF proteins are conserved stem cell regulators (25–27).

The mitotic region is patterned with respect to both the expression of certain key regulators as well as cell cycle properties (7, 12, 13, 16, 17, 20, 28–30). For example, meiotic S-phase begins in the proximal-most germ cells of the mitotic region (Fig. 1*A*), and GLD-1, a translational repressor that promotes meiotic entry, is barely detectable in the distal mitotic region, but becomes easily detectable in the midmitotic region and abundant once germ cells have entered meiotic prophase (Fig. 1*D*). These variations within the mitotic region raise the question of whether mitotically dividing germ cells also vary in their ability to differentiate and what mechanisms control that patterning. We have addressed this question by blocking cell movement and asking whether, with time, germ cells at different positions in the mitotic region progress toward meiotic entry or remain in an immature, undifferentiated state. Our results identify two pools within the mitotic region. Germ cells in a distal pool, defined by position close to the DTC niche, exist in an immature and essentially uniform state with respect to differentiation, whereas germ cells in a more proximal pool have begun to mature and are organized in a distal to proximal gradient of maturity. We discuss the existence and properties of these two pools in light of knowledge of the regulatory network controlling self-renewal and early differentiation.

Results

Two Pools Within the Mitotic Region Have Distinct Properties. To ask whether all mitotically dividing germ cells are equivalent in their capacity to enter meiosis, we stopped germ cell movement and scored meiotic prophase over time at fixed positions relative to the

Author contributions: O.C., S.L.C., and J.K. designed research; O.C., S.L.C., and D.E.M. performed research; O.C., S.L.C., D.E.M., and J.K. analyzed data; and O.C., S.L.C., and J.K. wrote the paper.

The authors declare no conflict of interest.

Freely available online through the PNAS open access option.

[1]O.C. and S.L.C. contributed equally to this work.

[2]To whom correspondence may be addressed. E-mail: ocinquin@uci.edu or jekimble@wisc.edu.

This article contains supporting information online at www.pnas.org/cgi/content/full/0912704107/DCSupplemental.

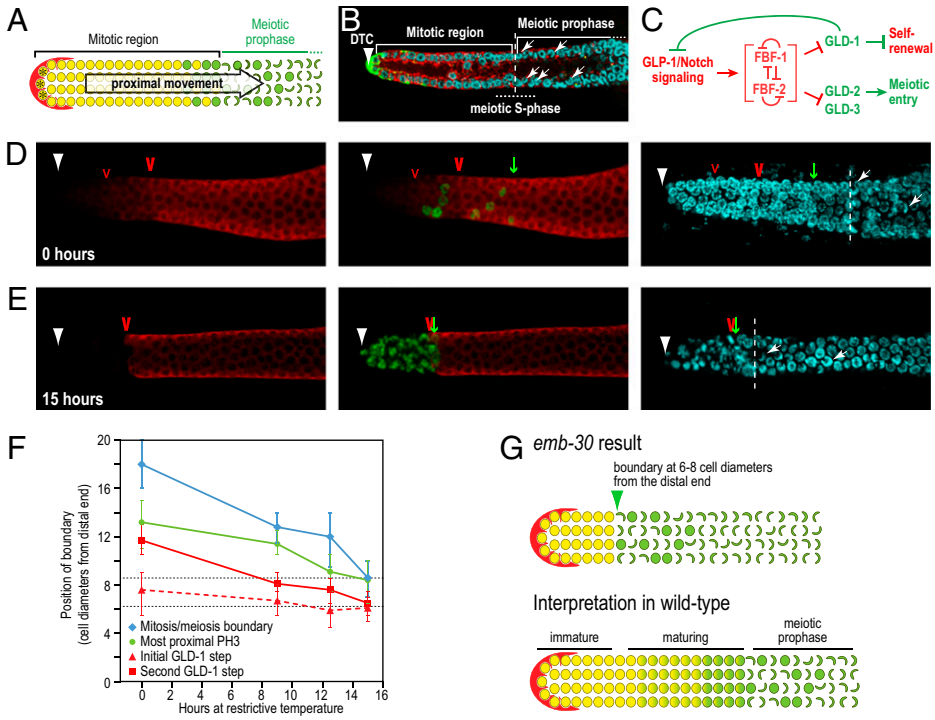

Fig. 1. Two pools with distinct differentiation capacities in the mitotic region. (*A*) Schematic of adult hermaphrodite distal gonad. Red, DTC; yellow circles, germ cells in mitotic cell cycle; *, inferred actual stem cells; green circles, germ cells in meiotic S-phase; green crescents, germ cells in early meiotic prophase. Movement through the mitotic region is inferred by the continuous movement of germ cells from the mitotic region to more proximal regions. Neighboring germ cells are often in distinct phases of the cell cycle. (*B, D,* and *E*) Confocal images of adult distal gonads. Dashed line, boundary between mitotic region and early meiotic prophase (the boundary is not always straight; it is drawn as a straight line for simplicity); dotted line, likely position of meiotic S phase; white arrowhead, distal end; white arrows, crescent-shaped DNA typical of meiotic prophase. (*B*) Wild-type distal gonad, single confocal section. DTC is stained with antibodies to GFP (green), germ-line membranes with antibodies to the GLP-1/Notch receptor (red), and DNA with DAPI (blue). (*C*) Simplified regulatory network for control of decision between self-renewal or early differentiation (meiotic entry). (*D* and *E*) Confocal projections of distal *emb-30* gonads at permissive temperature (*D*) [note that the most proximal PH3 in this germ line is not at the average position (see Fig. 1*F*)] and 15 h after a shift to restrictive temperature (*E*). Blue, DAPI-stained DNA; red, GLD-1; green, anti-PH3; small red carat, initial GLD-1 step; large red carat, second GLD-1 step; green arrow, most proximal mitotic division (PH3). *D* and *E* each show the same germ line with different fluorophores in *Left, Center,* and *Right*. (*F*) Position of key features in mitotic region with time after *emb-30* shift to restrictive temperature. Error bars represent 95% confidence intervals. Black dotted lines mark the rough boundary (6-8 gcd) between the distal and proximal pools. (*G*) Summary diagrams.

DTC. This analysis probes germ cell behavior in the presence of the DTC and Notch signaling. To stop movement, we used *emb-30(ts)*, a temperature-sensitive mutation that blocks the metaphase-to-anaphase transition at restrictive temperature (25 °C) (31). To confirm the movement block, we examined germ-line nuclei labeled with the thymidine analog EdU, over time. Whereas all EdU labeling moved proximally in wild-type germ lines at both 20 °C and 25 °C (7), label did not move in *emb-30* mutants after their shift to restrictive temperature. At both 9 h and 24 h after the shift, the most proximal EdU occurred at a similar position, measured in germ cell diameters from the distal end (gcd) [9 h was 24 gcd, 95% median confidence interval: 23–26 gcd, $n = 20$; 24 h was 23 gcd, 95% median confidence interval: 20–26 gcd, $n = 11$).

At permissive temperature (15 °C), distal germ lines from *emb-30* adults were similar to wild-type with respect to mitotic region size and GLD-1 accumulation (Fig. 1 *D* and *F*). By contrast, at restrictive temperature (25 °C), two distinct domains emerged where the mitotic region had been (Fig. 1 *E* and *G*). A distal pool of germ cells failed to up-regulate the GLD-1 and HIM-3 differentiation markers, failed to enter the meiotic cell cycle, and accumulated metaphase-arrested cells, whereas the proximal pool of germ cells accumulated GLD-1 and HIM-3 and entered meiotic prophase (Fig. 1*E*; Fig. S1*A*). Because the more proximal germ cells failed to arrest, their maturation into meiotic prophase likely circumvents mitotic arrest (see *Discussion*). Germ cells in these two pools therefore differed dramatically in their capacity to enter meiosis.

To examine formation of the boundary between the two pools, we scored *emb-30* germ lines at timed intervals (9, 12.5, and 15 h) after the shift. By 15 h, some germ lines (4/15) had some severely abnormal nuclei, making them difficult to score; therefore, we did not take later time points. Figs. 1 *D* and *E* show germ lines from the 0 and 15 h time points; Fig. S1 *B–E* shows the full time course; and Fig. 1*F* presents the cumulative data. At 15 °C, GLD-1 increased in the *emb-30* midmitotic region, usually in two steps—the initial one at 8 gcd on average and the second at 12 gcd on average (Fig. 1 *D Left* and *F*); the most proximal PH3-positive nucleus occurred at ≈13 gcd on average (Fig. 1 *D Center* and *F*), and the mitotic region extended to 18 gcd, on average (Fig. 1 *D Right* and *F*). We also measured these same features in microns and found their relative positions similar to those scored in gcd (Fig. S1*F*). In shifted *emb-30* germ lines, the position of the initial GLD-1 border did not change significantly between 0 and 15 h ($P > 0.16$), whereas the positions of the second GLD-1 border, the most proximal anti-PH3-positive nucleus and meiotic entry all moved distally ($P < 3.1 \times 10^{-6}$, $P < 1.4 \times 10^{-4}$, and $P < 4.2 \times 10^{-5}$, respectively) and finally came close to converging between 12.5 and 15 h. By 15 h after the shift, the position of meiotic entry and the proximal PH3 boundary were both found at 8 gcd, on average. The GLD-1 boundary was slightly more distal at 6 gcd, on average (Fig. 1*F*). All these features converged to a single site in some germ lines (20% at 12.5 h and ≈30% at 15 h). We conclude that the boundary between the two pools occurs at

6–8 gcd (Fig. 1*F*, black dotted lines). This boundary corresponds well to the position of the first GLD-1 step in unshifted animals (Fig. 1*D*, small red carat). The number of distal pool nuclei was ≈45 at both 12.5 h (average of 46; range of 26–86; 95% median confidence interval 36.5–56) and 15 h (average of 45; range of 24–66; 95% median confidence interval 31–57.5). The number of cells occupying the first six to eight rows in a wild-type germ line is 50–70 and, therefore, we estimate that the number of cells in a wild-type distal pool is likely to be 45–70.

Based on the two domains observed in shifted *emb-30* mutants, we suggest that maturation state varies among the ≈200 mitotically dividing germ cells and does so as a function of their position relative to the distal end. Cells in the distal pool were prevented from entering meiosis and appeared immature; cells in the proximal pool entered meiotic prophase, even in the presence of the DTC and Notch signaling. Moreover, because the proximal pool cells entered meiotic prophase progressively (Fig. 1*F*, blue line), we also suggest that a maturation gradient exists within the proximal pool (Fig. 1*G*).

The DTC Maintains a Distal Pool in an Immature State. To test whether the distal pool of germ cells in shifted *emb-30* mutants was maintained in an immature state, rather than being in an abnormal state that precludes maturation, we asked if they could enter meiotic prophase upon DTC removal. To this end, we first shifted *emb-30* adults to 25 °C, waited 9 h, ablated the DTC, and finally scored germ lines after a further 12 h at 25 °C (Fig. 2*A*). In unablated controls, the distal germ cells did not enter meiosis, as assayed by absence of abundant GLD-1 (100%, $n = 4$; Fig. 2*B*), absence of crescent-shaped DNA (100%, $n = 10$; Fig. 2*B*), and absence of chromosomal HIM-3 (100%, $n = 6$). By contrast, when the DTC was ablated, the distal germ cells accumulated abundant GLD-1 (100%, $n = 5$; Fig. 2*C*) and entered meiotic prophase, as assayed by both crescent-shaped DNA (100%, $n = 9$) and HIM-3 localization (100%, $n = 4$; Fig. 2*D*). We do not understand the mechanism by which germ cells escape cell cycle arrest after DTC ablation, but note that some nuclei with crescent-shaped DNA and chromosomal HIM-3 had not undergone DNA synthesis after DTC ablation (see *Methods*, Fig. 2*E*). Therefore, these cells appear to have progressed from their cell cycle arrest to meiotic prophase without DNA replication. We conclude that the arrested distal mitotic region cells are maintained in an immature state by DTC signaling and can differentiate in the absence of DTC signaling.

Removal of Notch Signaling Also Reveals Two Pools in the Mitotic Region. We next tested the state of maturity of germ cells in the mitotic region by a complementary method. Previous studies showed that Notch removal permits meiotic entry throughout the mitotic region (11). Because relatively immature cells should take longer to enter meiotic prophase than more mature cells, the time taken to enter meiotic prophase after Notch removal should provide a useful measure of germ cell maturity. Based on the *emb-30* results, we predicted that germ cells in the distal pool would be most immature and would therefore take longer to enter meiotic prophase than those in the proximal pool. We also predicted that germ cells in the proximal pool would enter meiosis in a spatiotemporal wave.

We removed Notch signaling by using a temperature-sensitive mutation in *glp-1*, which encodes the Notch receptor for germ line self-renewal. After shifting *glp-1(ts)* adults to restrictive temperature, we measured the time required before appearance of meiotic prophase nuclei as a function of position within the mitotic region. At permissive temperature (15 °C), *glp-1(ts)* germ lines entered meiotic prophase at ≈12 gcd (Fig. 3 *A* and *D*). After shifting to 25 °C, the average position of meiotic entry progressed gradually from ≈12 to ≈5 gcd over the first five hourly intervals (Fig. 3 *B–D*). This proximal-to-distal wave of meiotic entry is similar to the distal shift in meiotic entry seen in the proximal pool of shifted *emb-30* germ lines (Fig. 1*F*). By contrast, more distal germ cells (rows 1–5) had entered meiosis by 5.5 h after the shift to 25 °C (Fig. 3 *B–D*). Thus, germ cells in the distal pool entered meiosis in close synchrony. Moreover, germ cells in the distal pool entered meiosis after the proximal pool, confirming their relative immaturity. The close synchrony of meiotic entry in the distal pool suggests that those germ cells are maintained in an essentially uniform state.

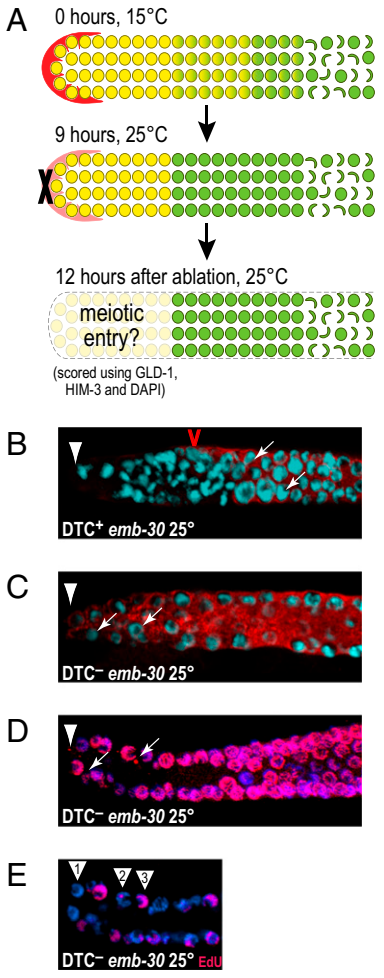

Fig. 2. The DTC maintains the *emb-30* distal pool in an immature state. (*A*) Experimental design. (*B-D*) Projections of confocal sections. White arrowhead marks distal end of gonad; white arrows mark meiotic prophase nuclei. (*B*) Unablated *emb-30* gonad incubated at 25 °C for 21 h. Nuclei are degenerating. GLD-1 (red); DAPI (cyan). Red carat marks GLD-1 border. (*C–E*) Ablated *emb-30* gonads. (*C*) GLD-1 (red); DAPI (cyan). (*D*) Chromosomal HIM-3 (pink); DAPI (blue). (*E*) EdU (pink, labeled for 12 h at 25 °C after ablation); DAPI (blue). Not all meiotic prophase nuclei contain EdU. Arrowheads: 1, no labeling with EdU; 2, weakly labeled with EdU; 3, well labeled with EdU.

Thus, two pools emerge in the *glp-1* experiments: a distal pool with cells in an immature state and a proximal pool with cells that are maturing in a wave. In the *glp-1* experiment, the distal pool contains 29 germ cells on average (range of 25–35, 95% median confidence interval 27–30), whereas the corresponding region in wild-type animals contains 40 germ cells on average. Although the sizes of the distal pools observed in the *emb-30* and *glp-1* experiments were not identical, they were roughly similar. We conclude that both *emb-30* and *glp-1* experiments identify two pools of germ cells within the mitotic region, a distal immature pool and a proximal maturing pool.

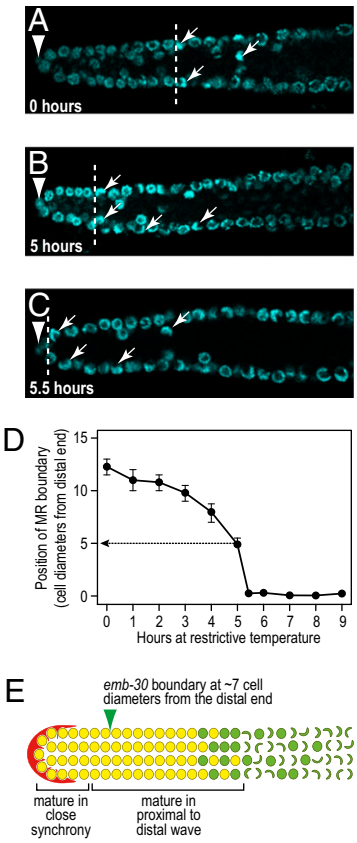

Fig. 3. Removal of Notch signaling reveals two pools within the mitotic region. (*A*-*C*) Distal gonads from *glp-1(ts)* adults grown at permissive temperature (*A*) or at restrictive temperature for the indicated times (*B* and *C*). Conventions as in Fig. 1. (*D*) Graph showing the position of meiotic entry as a function of time after *glp-1(ts)* adults were shifted to restrictive temperature. Error bars represent 95% median confidence intervals. (*E*) Summary diagram. The boundary between distal and proximal pools is similar although not identical in *glp-1* (brackets) and *emb-30* (green arrowhead) experiments (Fig. 1).

Discussion

We have identified two pools within the mitotic region of the *C. elegans* germ line. A distal pool exists in an essentially uniform state of immaturity, and a proximal pool has begun to mature toward differentiation (Fig. 4*A*). Here we discuss those two pools in light of previous analyses, including the molecular network controlling the decision between germ-line self-renewal and early differentiation. We propose a simple model to explain how cells are controlled to progress from a stem cell state to early differentiation (Fig. 4*B*).

The Distal Pool Is Composed of Stem Cell–Like Cells. The distal pool contains the most immature cells in the entire germ-line tissue and the DTC maintains that distal pool in its immature state. We suggest that this pool is in a stem cell–like state. The distal pool comprises ≈30–70 germ cells, which all behave similarly in the assays reported here. Despite this similar behavior, heterogeneities exist within the distal pool in terms of cell cycle properties (29), FBF-1 expression (12), and DTC contact (7). In addition, it seems likely that a hierarchical lineage relationship exists among cells in the distal pool. We previously inferred that cells immediately adjacent to the DTC body are likely to be actual stem cells, which generate more actual stem cells plus cells destined to differentiate (7); lineaging experiments to test this idea are not yet technically feasible. Our discovery of the distal pool of cells maintained in an essentially equivalent immature state suggests that the daughters generated by the actual stem cells are maintained as potential stem cells, as discussed in Potten and Loeffler (10). Thus the stem cell pool likely consists of both actual and potential stem cells. Heterogeneity among cells with self-renewal potential exists in other systems as well (2, 32–34).

According to our model, germ cells are triggered to leave the stem cell–like state when they move from the distal pool to the proximal pool (Fig. 4*B*). The position of that trigger determines the size of the distal pool, which we predict to be ≈30–70 germ cells in a wild-type germ line. This rough number is consistent with the ≈35 germ cells recently found to regenerate a complete and functional adult germ line after starvation (35). We note that our distal pool and the ≈35 cell pool found by Angelo and Van Gilst were defined by different assays and that the optimal number of germ cells preserved upon starvation may not precisely match the optimal number of cells kept in a stem cell–like state under well-fed conditions. The molecular basis of the trigger to leave the stem cell state is not understood. One plausible mechanism is a drop in Notch signaling that might occur after loss of physical contact with the DTC niche. This drop in signaling •••, in turn, would trigger a change in the network and begin the transition from a stem cell–like state to an early differentiated state (Fig. 4*A*).

The Proximal Pool Contains Transit-Amplifying Cells. Germ cells in the proximal pool are more mature than those in the distal pool, and they enter meiotic prophase despite the presence of the DTC if a cell cycle block is imposed to stop movement. We suggest that germ cells normally commit to maturation when they leave the distal pool. It is possible that *emb-30* removal may affect cell fates in addition to its effect on cell movement (for example, by eliciting different checkpoint responses in distal and proximal pools or by directly controlling regulator activity). Testing whether such effects occur and whether they contribute to the distinction between the two pools awaits further experiments.

Maturation in the proximal pool is graded, with the more distal cells in the pool being less mature than the more proximal ones. The distal to proximal maturation gradient suggests that progression from the stem cell state to the early differentiation state may be controlled by a timing mechanism, for example by the kinetics of the network transition between modes. Similar timing mechanisms have been proposed in a wide variety of experimental systems (8). At the current time, we do not know whether the timing mechanism relevant to *C. elegans* germ cells is entirely cell intrinsic or influenced by diffusion between the interconnected germ cells.

The germ cells in the proximal pool appear to be transit-amplifying cells (Fig. 4*B*). Transit-amplifying cells are defined in other systems as having left the stem cell state to mature while at the same time continuing to proliferate (10, 34, 36). The idea that the mitotic region may include transit-amplifying cells is not new (see, for example, refs. 6, 12, 29, and 37). These earlier works based this idea on expression of markers and cell cycle properties. Here, we have used two complementary assays to learn which germ cells have been triggered to mature and therefore have become committed to the maturation process. Although our model is that cells in the proximal pool are normally committed to mature, we emphasize that our work does not assay the potential of these cells to revert to a stem cell state. Such a potential for reversion is a strong possibility because in other systems, transit-amplifying cells can retain stem cell potential (38–41).

Network Control. Fig. 4*B* presents a simple model for how the network controlling germ-line self-renewal or meiotic entry may work in the distal and proximal pools of the mitotic region. This network can be viewed as existing in two modes, one driving

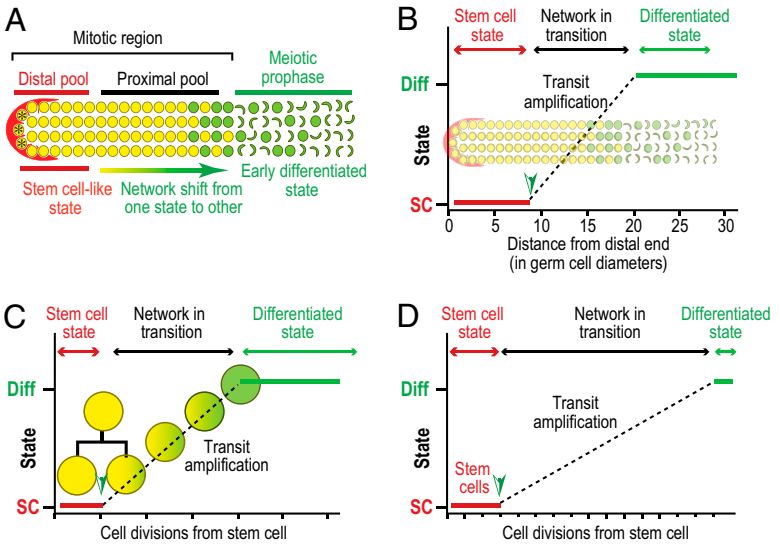

Fig. 4. Model for network control of the progression from stem cells through transit-amplifying cells and into early differentiation. (*A*) Two pools with distinct properties in the mitotic region. Germ cells in the distal pool are maintained in a stem cell–like state; germ cells in the proximal pool are maturing from the stem cell–like state to the early differentiated state. (*B–D*) Models for network control of the progression from stem cell to early differentiation in three different systems. The network transition between states is drawn as a line for simplicity. SC, stem cell state; Diff, early differentiated state; arrowhead, trigger to leave stem cell state and start network maturation toward the early differentiated state. (*B*) Model for network control of the *C. elegans* distal germ line. (*C*) Model for network control of a stem cell asymmetric division. (*D*) Model for network control of a vertebrate stem cell system that makes a large number of transit-amplifying cells.

germ-line self-renewal (Fig. 4*B*, red line) and the other driving early differentiation (meiotic entry) (Fig. 4*B*, green line). We suggest that cells in the distal pool reflect action of the self-renewal mode of the network and that cells entering overt meiotic prophase have reached its early differentiation mode. In between, in the proximal pool, the network transitions from one mode to the other (Fig. 4*B*, dotted line).

Two features of our model (Fig. 4*B*) are predicted to govern the sizes of the distal and proximal pools. Distal pool size relies on the position of the trigger that drives the network to leave its self-renewal mode (Fig. 4*B*, arrowhead). That position is likely controlled by DTC position, either directly (loss of DTC contact) or indirectly (change in network due to distance from DTC contact). By contrast, the proximal pool size relies, at least in part, on a "maturation timer" that reflects the kinetics of the transition from one network mode to the other (Fig. 4*B*). Other factors are also critical (e.g., cell cycle rate). Although the maturation timer idea must be tested by using molecular measures of network kinetics, which we do not yet have, it provides a simple explanation for the progression from stem cell to early differentiation in terms of network dynamics. Indeed, if the proximal pool is controlled in a manner analogous to transit-amplifying cells, this concept may also help explain the control of this pool in vertebrates.

Our model for the network control of stem cells and their progeny provides a useful framework for thinking about the plasticity of stem cell controls, both in *C. elegans* and more generally. By modifying network parameters, the stem cell and transit-amplifying pools can be either increased or decreased in response to physiological, environmental, clinical, or evolutionary challenges. Moreover, if the trigger were positioned close to the niche, an asymmetric stem cell division could result (Fig. 4*C*), or if the kinetics of the transition between network modes were sufficiently slowed, a virtually unregulated transit amplification could result (Fig. 4*D*). Therefore, understanding the network control of *C. elegans* germ-line stem cells can serve as a paradigm for understanding more broadly how a network controls stem cells and may have implications for human disease.

Methods

Worm Maintenance. Strains were maintained as described in ref. 42, at 15 °C [permissive temperature for *glp-1(q224)* and *emb-30(tn377)*] or 20 °C (all other strains). Shifts to restrictive temperature were done with animals grown at 15 °C until 36 h past L4 by moving plates to a 25 °C incubator or by using an EchoTherm timed incubator (Torrey Pines Scientific; incubator temperature shift occurred in less than 3 min). Animals at 15 °C were examined at 36 h past stage L4. The wild-type strain was N2 Bristol.

DTC Ablations. Laser ablations were performed as described in ref. 43 in *emb-30; qIs56*, whose DTCs express GFP (44). Room temperature was maintained at 25 °C during the entire ablation process. Only worms in which the DTC cytoplasm was observed to ooze out of the cell as a result of ablation were further analyzed; ablations were further validated by nuclear and cellular morphology after microsurgery (ablation also led to a strong reduction or loss of GFP signal after 24 h of incubation). Only 1 gonadal arm was ablated per worm; the unablated arm served as a control.

EdU Labeling After Ablation. To assay germ cell cycle behavior after DTC ablation, *emb-30* animals were shifted to 25 °C for 9 h, DTCs were ablated and animals were further incubated for 12 h at 25°C on agar plates seeded with *Escherichia coli* labeled with 1 μM EdU. EdU is a thymidine analog whose incorporation can be used like BrdU to label cells undergoing DNA replication (45); EdU-labeled cells were stained with a Click-iT EdU Alexa Fluor Imaging Kit (Invitrogen, Eugene, OR).

Antibody Staining. Antibody and DAPI staining were performed on extruded germ lines as described in ref. 46. Germ lines were fixed with 2% PFA, permeabilized with 0.1–0.4% Triton X-100 and imaged with a Zeiss LSM510 confocal microscope. Antibodies were anti-PH3, 1:200 (Upstate Biotechnology, Lake Placid, NY) (12); anti-HIM-3, 1:500 (47); and anti-GLD-1, 1:100 (gift of E. Goodwin, Department of Genetics, University of Wisconsin-Madison). GLD-1 and PH3 images in Fig. 1 are average non-0 projections done with a customized version of ImageJ. DAPI images in Fig. 1 are maximum intensity projections of ≈5 focal planes done with ImageJ.

Scoring GLD-1 Boundaries. GLD-1 boundaries were marked in ImageJ by scrolling through z-series and drawing a line through the boundary. Position to the GLD-1 boundary was determined by counting number of DAPI-stained nuclei (gcd) or by measuring the distance (microns) between the line and the distal end of the germ line. When the GLD-1 boundary was not straight across, the average of distal- and proximal-most edges of the boundary was estimated.

Counting Germ Cells in Distal Domain. To estimate the number of cells in the distal pool, we counted nuclei distal to the GLD-1 border. We consider this an estimate because metaphase arrest and abnormal nuclear morphology made counting difficult. The number of cells arrested in metaphase after shifting *emb-30* was variable, which could also contribute to the variability in our counts.

Statistics. All calculations were performed by using R (http://r-project.org). The asymptotic Wilcoxon rank sum test was used for pairwise comparisons (two-sided tests) and to derive median confidence intervals.

ACKNOWLEDGMENTS. We thank Tim Schedl and Betsy Goodwin for reagents, the *Caenorhabditis* Genetics Center, funded by the NIH National Center for Research Resources, for providing nematode strains, Jadwiga Forster and Peggy Kroll-Conner for technical help, Josh Snow, members of the J.K. laboratory and Amanda Cinquin for discussions, Amanda Cinquin for help analyzing data, Susan Strome and David Greenstein for helpful comments, Anne Helsley-Marchbanks and Laura Vanderploeg for help preparing the manuscript and figures, and the University of California, Irvine Optical Biology Core Facility for microscopy resources. O.C. thanks the University of California, Irvine for startup funds. D.E.M. was supported by NIH Training Grant T32 GM07215 in Molecular Biosciences. NIH Grant GM069454 (to J.K.) supported this work. J.K. is an investigator with the Howard Hughes Medical Institute.

1. Li L, Xie T (2005) Stem cell niche: Structure and function. *Annu Rev Cell Dev Biol* 21: 605–631.
2. Morrison SJ, Spradling AC (2008) Stem cells and niches: Mechanisms that promote stem cell maintenance throughout life. *Cell* 132:598–611.
3. Knoblich JA (2008) Mechanisms of asymmetric stem cell division. *Cell* 132:583–597.
4. Morrison SJ, Kimble J (2006) Asymmetric and symmetric stem-cell divisions in development and cancer. *Nature* 441:1068–1074.
5. Kimble J, Crittenden SL (2007) Controls of germline stem cells, entry into meiosis, and the sperm/oocyte decision in *Caenorhabditis elegans*. *Annu Rev Cell Dev Biol* 23: 405–433.
6. Hubbard EJ (2007) *Caenorhabditis elegans* germ line: A model for stem cell biology. *Dev Dyn* 236:3343–3357.
7. Crittenden SL, Leonhard KA, Byrd DT, Kimble J (2006) Cellular analyses of the mitotic region in the *Caenorhabditis elegans* adult germ line. *Mol Biol Cell* 17:3051–3061.
8. Cinquin O (2009) Purpose and regulation of stem cells: A systems-biology view from the *Caenorhabditis elegans* germ line. *J Pathol* 217:186–198.
9. Aherne WA, Camplejohn RS, Wright NA (1977) *An Introduction to Cell Population Kinetics* (Edward Arnold Ltd, London).
10. Potten CS, Loeffler M (1990) Stem cells: Attributes, cycles, spirals, pitfalls and uncertainties. Lessons for and from the crypt. *Development* 110:1001–1020.
11. Austin J, Kimble J (1987) *glp-1* is required in the germ line for regulation of the decision between mitosis and meiosis in C. elegans. *Cell* 51:589–599.
12. Crittenden SL, et al. (2002) A conserved RNA-binding protein controls germline stem cells in *Caenorhabditis elegans*. *Nature* 417:660–663.
13. Lamont LB, Crittenden SL, Bernstein D, Wickens M, Kimble J (2004) FBF-1 and FBF-2 regulate the size of the mitotic region in the *C. elegans* germline. *Dev Cell* 7:697–707.
14. Francis R, Barton MK, Kimble J, Schedl T (1995) *gld-1*, a tumor suppressor gene required for oocyte development in *Caenorhabditis elegans*. *Genetics* 139:579–606.
15. Kadyk LC, Kimble J (1998) Genetic regulation of entry into meiosis in *Caenorhabditis elegans*. *Development* 125:1803–1813.
16. Eckmann CR, Crittenden SL, Suh N, Kimble J (2004) GLD-3 and control of the mitosis/meiosis decision in the germline of *Caenorhabditis elegans*. *Genetics* 168:147–160.
17. Hansen D, Wilson-Berry L, Dang T, Schedl T (2004) Control of the proliferation versus meiotic development decision in the *C. elegans* germline through regulation of GLD-1 protein accumulation. *Development* 131:93–104.
18. Jones AR, Schedl T (1995) Mutations in *gld-1*, a female germ cell-specific tumor suppressor gene in *Caenorhabditis elegans*, affect a conserved domain also found in Src-associated protein Sam68. *Genes Dev* 9:1491–1504.
19. Eckmann CR, Kraemer B, Wickens M, Kimble J (2002) GLD-3, a Bicaudal-C homolog that inhibits FBF to control germline sex determination in *C. elegans*. *Dev Cell* 3: 697–710.
20. Wang L, Eckmann CR, Kadyk LC, Wickens M, Kimble J (2002) A regulatory cytoplasmic poly(A) polymerase in *Caenorhabditis elegans*. *Nature* 419:312–316.
21. Jan E, Motzny CK, Graves LE, Goodwin EB (1999) The STAR protein, GLD-1, is a translational regulator of sexual identity in *Caenorhabditis elegans*. *EMBO J* 18: 258–269.
22. Suh N, Jedamzik B, Eckmann CR, Wickens M, Kimble J (2006) The GLD-2 poly(A) polymerase activates *gld-1* mRNA in the *Caenorhabditis elegans* germ line. *Proc Natl Acad Sci USA* 103:15108–15112.
23. Berry LW, Westlund B, Schedl T (1997) Germ-line tumor formation caused by activation of *glp-1*, a *Caenorhabditis elegans* member of the *Notch* family of receptors. *Development* 124:925–936.
24. Hansen D, Hubbard EJA, Schedl T (2004) Multi-pathway control of the proliferation versus meiotic development decision in the *Caenorhabditis elegans* germline. *Dev Biol* 268:342–357.
25. Chiba S (2006) Notch signaling in stem cell systems. *Stem Cells* 24:2437–2447.
26. Wickens M, Bernstein DS, Kimble J, Parker R (2002) A PUF family portrait: 3′ UTR regulation as a way of life. *Trends Genet* 18:150–157.
27. Salvetti A, et al. (2005) *DjPum*, a homologue of *Drosophila Pumilio*, is essential to planarian stem cell maintenance. *Development* 132:1863–1874.
28. Jaramillo-Lambert A, Ellefson M, Villeneuve AM, Engebrecht J (2007) Differential timing of S phases, X chromosome replication, and meiotic prophase in the *C. elegans* germ line. *Dev Biol* 308:206–221.
29. Maciejowski J, Ugel N, Mishra B, Isopi M, Hubbard EJA (2006) Quantitative analysis of germline mitosis in adult *C. elegans*. *Dev Biol* 292:142–151.
30. Jones AR, Francis R, Schedl T (1996) GLD-1, a cytoplasmic protein essential for oocyte differentiation, shows stage- and sex-specific expression during *Caenorhabditis elegans* germline development. *Dev Biol* 180:165–183.
31. Furuta T, et al. (2000) EMB-30: An APC4 homologue required for metaphase-to-anaphase transitions during meiosis and mitosis in *Caenorhabditis elegans*. *Mol Biol Cell* 11:1401–1419.
32. Orkin SH, Zon LI (2008) Hematopoiesis: An evolving paradigm for stem cell biology. *Cell* 132:631–644.
33. Yoshida S (2009) Casting back to stem cells. *Nat Cell Biol* 11:118–120.
34. Fuchs E (2009) The tortoise and the hair: Slow-cycling cells in the stem cell race. *Cell* 137:811–819.
35. Angelo G, Van Gilst MR (2009) Starvation protects germline stem cells and extends reproductive longevity in *C. elegans*. *Science* 326:954–958.
36. Watt FM, Hogan BL (2000) Out of Eden: Stem cells and their niches. *Science* 287: 1427–1430.
37. Hansen D, Schedl T (2006) The regulatory network controlling the proliferation-meiotic entry decision in the *Caenorhabditis elegans* germ line. *Curr Top Dev Biol* 76: 185–215.
38. Doetsch F, Petreanu L, Caille I, Garcia-Verdugo J-M, Alvarez-Buylla A (2002) EGF converts transit-amplifying neurogenic precursors in the adult brain into multipotent stem cells. *Neuron* 36:1021–1034.
39. Brawley C, Matunis E (2004) Regeneration of male germline stem cells by spermatogonial dedifferentiation in vivo. *Science* 304:1331–1334.
40. Kai T, Spradling A (2004) Differentiating germ cells can revert into functional stem cells in *Drosophila melanogaster* ovaries. *Nature* 428:564–569.
41. Barroca V, et al. (2009) Mouse differentiating spermatogonia can generate germinal stem cells *in vivo*. *Nat Cell Biol* 11:190–196.
42. Brenner S (1974) The genetics of *Caenorhabditis elegans*. *Genetics* 77:71–94.
43. Bargmann CI, Avery L (1995) Laser killing of cells in Caenorhabditis elegans. *Caenorhabditis elegans: Modern Biological Analysis of an Organism, Methods in Cell Biology*, eds Epstein HF, Shakes DC (Academic, San Diego), pp 225–250.
44. Blelloch R, et al. (1999) The *gon-1* gene is required for gonadal morphogenesis in *Caenorhabditis elegans*. *Dev Biol* 216:382–393.
45. Salic A, Mitchison TJ (2008) A chemical method for fast and sensitive detection of DNA synthesis *in vivo*. *Proc Natl Acad Sci USA* 105:2415–2420.
46. Crittenden SL, Kimble J (2008) Analysis of the C. elegans germline stem cell region. *Germline Stem Cell Protocols, Methods in Molecular Biology*, eds Hou S, Singh SR (Humana, Totowa, NJ), Vol 450, pp 27–44.
47. Zetka MC, Kawasaki I, Strome S, Müller F (1999) Synapsis and chiasma formation in *Caenorhabditis elegans* require HIM-3, a meiotic chromosome core component that functions in chromosome segregation. *Genes Dev* 13:2258–2270.